

Storage Ring Measurement of the Proton Electric Dipole Moment

Richard Talman
Laboratory for Elementary-Particle Physics
Cornell University

11 October, 2017, CERN

2 Outline

EDM and symmetry violation—You have heard this before, but not today

Capsule history of force field symmetries

Why measure EDM?—You have heard this before, but not today

Why all-electric ring?

Two experiments that “could not be done”

EDM precision goals—space domain or frequency domain method

Planned Jefferson Lab Stern-Gerlach electron polarimetry test(s)

Design requirements for proton EDM storage ring, e.g. at CERN

Weak-weaker WW-AG-CF focusing ring design

Total drift length condition for below-transition operation

Longitudinal γ variation on off-momentum orbits

Potential energy

Ultraweak focusing

Parameter table

Lattice functions

Self-magnetometry

Virial theorem decoherence calc. decoherence \sim focusing-strength

The Brookhaven “AGS-Analogue” electrostatic ring

Heading only—***Run-duration limiting factors***

Mundane storage ring loss mechanisms

Spin decoherence

Polarimetry beam consumption

Heading only—***Phase-locked “Penning-like” trap operation***

Heading only—***Stochastic cooling stabilization of IBS ?***

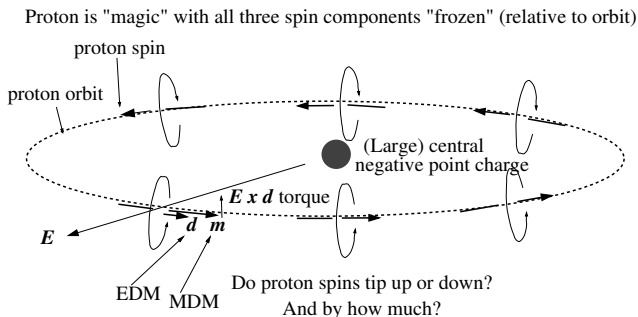
3 Capsule history of force field symmetries

- ▶ Newton: Gravitational field, (inverse square law) central force
- ▶ Coulomb: By analogy, electric force is the same (i.e. central, $1/r^2$)
- ▶ Ampere: How can compass needle near a current figure out which way to turn? Magnetic field is **pseudo-vector**. A **right hand rule** is somehow built into E&M and into the compass needle.
- ▶ The upshot: by introducing **pseudo-vector** magnetic field, E&M respects reflection symmetry. This was the first step toward the **grand unification** of all forces.
- ▶ Lee, Yang, etc: A particle with spin (**pseudo-vector**), say “up”, can decay more up than down (**vector**);
 - ▶ i.e. the decay vector is parallel (not anti-parallel) to the spin pseudo-vector,
 - ▶ viewed in a mirror, this statement is reversed.
 - ▶ i.e. weak decay force violates reflection symmetry (P).
- ▶ Fitch, Cronin, etc: standard model violates both parity (P) and time reversal (T), so protons, etc. must have both MDM and EDM
- ▶ Current task: How to exploit the implied symmetry violation to measure the EDM of proton, electron, etc?

4 Why all-electric ring?

- ▶ “Frozen spin” operation in all-electric storage ring is only possible with electrons or protons—by chance their anomalous magnetic moment values are appropriate. The “magic” kinetic energies are 14.5 MeV for e, 233 MeV for p.
- ▶ Beam direction reversal is possible in all-electric storage ring, with all parameters except injection direction held fixed. This is crucial for reducing systematic errors.

5 EDM Sensitive Configuration—modern day Ampère experiment



Two issues:

- ▶ Can the tipping angle be measurably large for plausibly large EDM, such as 10^{-30} e-cm? With modern technology, yes
- ▶ Can the symmetry be adequately preserved when the idealized configuration above is approximated in the laboratory? *This is the main issue*

6 Two experiments that “could not be done”

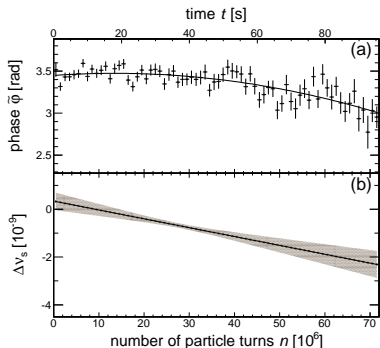


FIG. 3. (a): Phase $\tilde{\varphi}$ as a function of turn number n for all 72 turn intervals of a single measurement cycle for $\nu_s^{\text{fix}} = -0.160975407$, together with a parabolic fit. (b): Deviation $\Delta\nu_s$ of the spin tune from ν_s^{fix} as a function of turn number in the cycle. At $t \approx 38$ s, the interpolated spin tune amounts to $\nu_s = (-16097540771.7 \pm 9.7) \times 10^{-11}$. The error band shows the statistical error obtained from the parabolic fit, shown in panel (a).

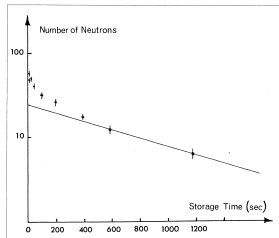
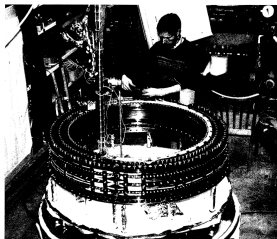


Figure: COSY, Juelich, Eversmann et al.: (Pseudo-)frozen spin deuterons, and Bonn, Paul et al.: neutron storage ring

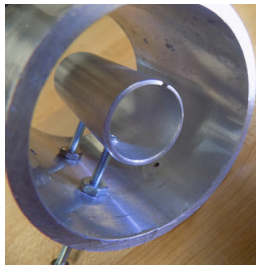
7 Precision limit—space domain method

- ▶ Measure difference of beam polarization orientation at end of run minus at beginning of run.
- ▶ p-Carbon left/right scattering asymmetry polarimetry.
- ▶ This polarimetry is well-tested, “guaranteed” to work,
- ▶ but also “destructive” (measurement consumes beam)

particle	$ d_{elec} $ current upper limit e-cm	error after 10^4 pairs of runs e-cm
neutron	3×10^{-26}	
proton	8×10^{-25}	$\pm 10^{-29}$
electron	10^{-28}	$\pm 10^{-29}$

8 Resonant polarimetry

- ▶ Planned Stern-Gerlach electron polarimetry test(s)
- ▶ R. Talman, LEPP, Cornell University;
B. Roberts, University of New Mexico;
J. Grames, A. Hofler, R. Kazimi, M. Poelker, R. Suleiman;
Thomas Jefferson National Laboratory
2017 International Workshop on Polarized Sources,
Targets & Polarimetry,
Oct 16-20, 2017,



9 Precision limit—frequency domain method

- ▶ Frequency domain
- ▶ Measure the spin tune shift when EDM precession is reversed
- ▶ Relies on phase-locked Stern-Gerlach polarimetry
- ▶ Like the Ramsey neutron EDM method.
- ▶ This polarimetry has not yet been proven to work.
- ▶ **This method cannot be counted on until resonant polarimetry has been shown to be practical.**

particle	$ d_{\text{elec}} $ current upper limit e-cm	excess fractional cycles per pair of 1000 s runs	error after 10^4 pairs of runs e-cm	roll reversal error e-cm
neutron	3×10^{-26}	$\pm 8 \times 10^3$ ± 1	$\pm 10^{-30}$ $\pm 10^{-30}$	$\pm 10^{-30}$ $\pm 10^{-30}$
proton	8×10^{-25}			
electron	10^{-28}			

10 Achievable precision (assuming perfect phase-lock)

- ▶ EDM in units of (nominal value) 10^{-29} e-cm $\equiv \tilde{d}$
- ▶ $2 \times \text{EDM}(\text{nominal})/\text{MDM}$ precession rate ratio:
 $2\eta^{(e)} = 0.92 \times 10^{-15} \approx 10^{-15}$
- ▶ duration of each one of a pair of runs = T_{run}
- ▶ smallest detectable fraction of a cycle = $\eta_{\text{fringe}} = 0.001$

$$N_{FF} = \text{EDM induced fractional fringe shift per pair of runs}$$
$$= \frac{(2\eta^{(e)})\tilde{d}}{\eta_{\text{fringe}}} h_r f_0 T_{\text{run}} \quad \left(\begin{array}{l} \text{e.g.} \\ \approx \tilde{d} \frac{10^{-15} \cdot 10 \cdot 10^7 \cdot 10^3}{10^{-3}} = 0.1\tilde{d} \end{array} \right),$$

Assumed roll rate reversal error : $\pm \eta^{\text{rev.}}$ e.g. 10^{-10}

$$\sigma_{FF}^{\text{rev.}} = \text{roll reversal error measured in fractional fringes}$$
$$= \pm \frac{f^{\text{roll}} \eta^{\text{rev.}} T_{\text{run}}}{\eta_{\text{fringe}}} \quad \left(\begin{array}{l} \text{e.g.} \\ \approx \pm \frac{10^2 \cdot 10^{-10} \cdot 10^3}{10^{-3}} = 10^{-2} \end{array} \right).$$

11 Design requirements for proton EDM storage ring, e.g. at CERN

- ▶ Measuring the proton electric dipole moment (EDM) requires an electrostatic storage ring in which 233 MeV, frozen spin polarized protons can be stored for an hour or longer without depolarization.
- ▶ The design orbit consists of multiple electrostatic circular arcs
 - ▶ Electric breakdown limits bending radius, e.g. $r_0 > 40$ m
 - ▶ For longest spin coherence time (SCT) and for best systematic error reduction the *focusing needs to be as weak as possible*
 - ▶ This is a “worst case” condition for electric and magnetic storage rings to differ (because kinetic energy depends on electric potential energy)
 - ▶ To reduce emittance dilution by intrabeam scattering (IBS) the ring needs to operate “below transition”
- ▶ Ring must be accurately clockwise/counter-clockwise symmetric
 - ▶ Accurately symmetric injection lines are required.
 - ▶ Initially single beams would be stored, with run-to-run alternation of circulation directions.
 - ▶ Ultimate reduction of systematic error will require simultaneously counter-circulating beams.

“Magic” central design parameters for frozen spin proton operation:

$$c = 2.99792458e8 \text{ m/s}$$

$$m_p c^2 = 0.93827231 \text{ GeV}$$

$$G = 1.7928474$$

$$g = 2G + 2 = 5.5856948$$

$$\gamma_0 = 1.248107349$$

$$\mathcal{E} = \gamma_0 m_p c^2 = 1.171064565 \text{ GeV}$$

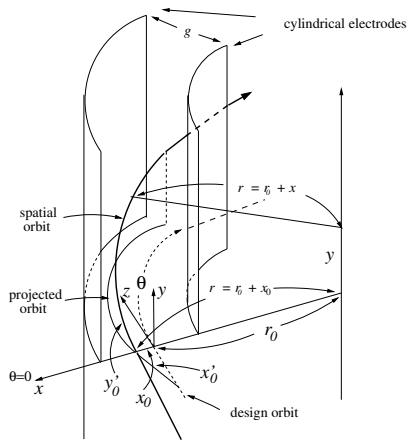
$$K_0 = \mathcal{E} - m_p c^2 = 0.232792255 \text{ GeV}$$

$$p_0 c = 0.7007405278 \text{ GeV}$$

$$\beta_0 = 0.5983790721$$

13 *Weak-weaker WW-AG-CF focusing* ring design

- ▶ An ultraweak focusing, “weak/weaker, alternating-gradient, combined-function” (WW-AG-CF) electric storage ring is described.
- ▶ All-electric bending fields exist in the tall slender gaps between inner and outer, vertically-plane, horizontally-curved electrodes.



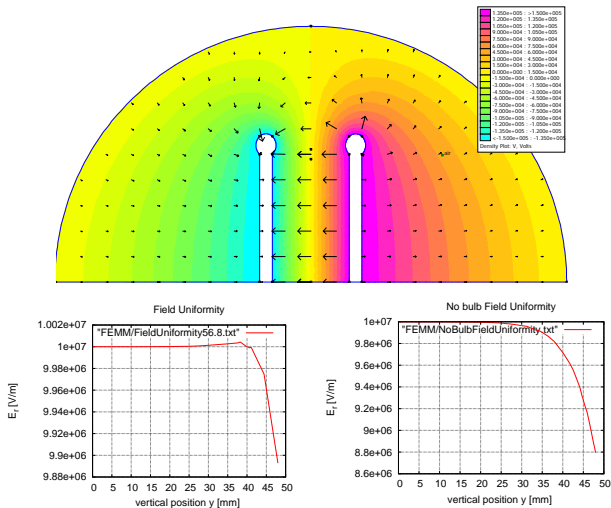


Figure: Above: Electrode edge shaping to maximize uniform field volume; Below left: bulb-corrected field uniformity; Below right: uncorrected field intensity. Only the top 5 cm is shown. The electrode height can be increased arbitrarily without altering the electric field.

- ▶ The radial electric field dependence is

$$E = E_r \sim \frac{1}{r^{1+m}},$$

where, ideally for spin decoherence, the field index m would be exactly $m = 0$.

- ▶ $m = 0$ (pure-cylindrical) field produces horizontal bending as well as horizontal “geometric” focusing, but no vertical force
- ▶ (Not quite parallel) electrodes, with m alternating between $m = -0.002$ and $m = +0.002$ provides net vertical focusing.
- ▶ Not “strong focusing”, this is “weak-weaker” WW-AG-CF focusing, just barely strong enough to keep particles captured vertically.
- ▶ Beam distributions are highly asymmetric, much higher than wide, matching the good field storage ring aperture.

- ▶ (Not counting trims, nor slanted poles) there are no quadrupoles
- ▶ This is favorable for systematic electric dipole moment (EDM) error reduction. *There is no spin decoherence (for frozen spins) in a pure $m = 0$ field* — explained later
- ▶ The average particle speeds in drift sections do not need to be magic—because there is no spin precession in drift sections.
- ▶ Still, the dependence of revolution period on momentum offset is very small, making the synchrotron oscillation frequency small, and not necessarily favorable as regards being above or below transition.
- ▶ IBS stability requires below-transition operation, which requires quite long total drift length.

17 Total drift length condition for below-transition operation

- ▶ As with race horses, faster particles can lose ground in the curves but still catch up in the straightaways.
- ▶ To run “below transition”, the sum of all drift lengths has to exceed $L_D^{\text{trans.}}$, given in terms of dispersion D^O by

$$L_D^{\text{trans.}} = 2\pi D^O \beta_0 \gamma_0 \approx 2\pi D^O.$$

18 Longitudinal γ variation on off-momentum orbits

Extreme off-momentum $\Delta\gamma$ (s) plots

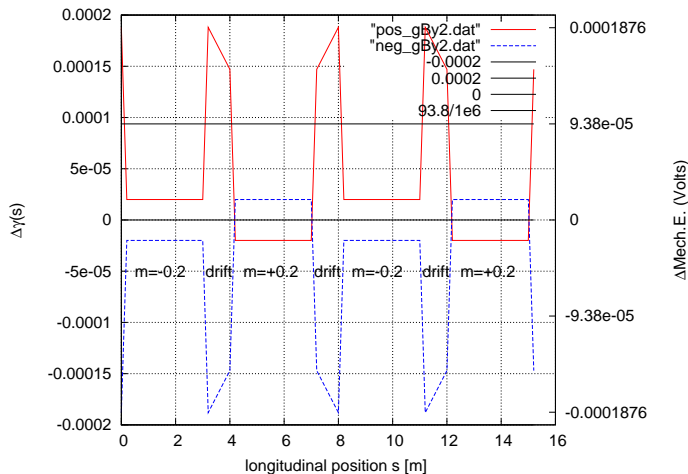


Figure: Dependence of deviation from "magic" $\Delta\gamma(s) = \gamma(s) - \gamma_0$ on longitudinal position s , for off-momentum closed orbits (circular arcs within bends) just touching inner or outer electrodes at $x = \pm 0.015$ m. Notice the anomalous cross-overs in $m > 0$ bends.

19 Off-momentum closed orbits

- ▶ For central radius r_0 the off-momentum radius is determined by Newton's centripetal force law

$$eE_0 \left(\frac{r_0}{r} \right)^{1+m} = \frac{\beta pc}{r} \stackrel{\text{also}}{=} \frac{m_p c^2}{r} \left(\gamma - \frac{1}{\gamma} \right),$$

where $r = r_0 + x_D$ is the radius of an off-momentum arc of a circle with the same center.

- ▶ For $m \neq 0$, r cancels, and the radius is indeterminate.
- ▶ A powerful coordinate transformation is:

$$\xi = \frac{x}{r} = \frac{x}{r_0 + x}$$

- ▶ For our typical values ($x = 1$ cm, $r_0 = 40$ m), for all practical purposes, ξ can simply be thought of as x in units of r_0 .

- ▶ The electric field is then

$$\mathbf{E}(\xi) = -E_0 (1 - \xi)^{1+m} \hat{\mathbf{r}},$$

- ▶ Off-momentum closed orbits are “parallel” arcs of radius $r = r_0 + x_D$ inside a bend, entering and exiting at right angles to straight line orbits displaced also by x_D .
- ▶ The relativistic gamma factor on the orbit (inside) is γ^I , which satisfies

$$eE_0 r_0 (1 - \xi)^m = \beta^I p^I c = m_p c^2 \left(\gamma^I - \frac{1}{\gamma^I} \right),$$

- ▶ This is a quadratic equation for γ^I *inside* bend.
- ▶ For $r \neq r_0$, because of the change in electric potential at the ends of a bend element, the gamma factor *outside* has a different value, γ^O .

- ▶ For $m \neq 0$ the orbit determination is no longer degenerate.
- ▶ Solving the quadratic equation for γ' , the gamma factor is given by the positive root;

$$\gamma'(\xi) = \frac{E_0 r_0 (1 - \xi)^m}{2m_p c^2 / e} + \sqrt{\left(\frac{E_0 r_0 (1 - \xi)^m}{2m_p c^2 / e} \right)^2 + 1}.$$

- ▶ This function is plotted next for $m = \pm 0.2$.

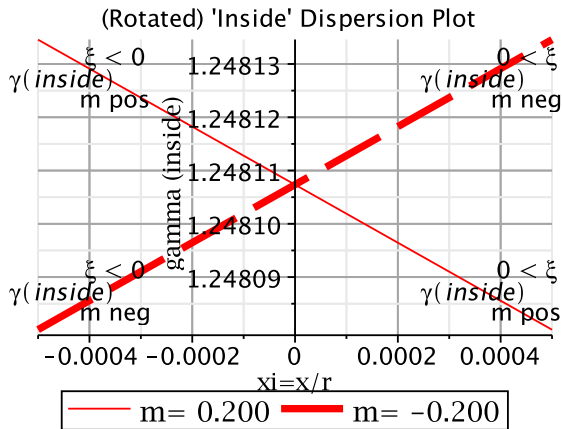


Figure: This figure shows a “dispersion plot” of “inside” gamma value γ^I plotted vs ξ . The curves intersect at the magic value $\gamma^I = 1.248107$. Because $d\gamma/d\beta = \beta\gamma^3$ is equal to about 1.17 at the magic proton momentum, the fractional spreads in velocity, momentum, and gamma are all comparable in value—in this case about $\pm 2 \times 10^{-5}$. This figure may be confusing, since it is rotated by 90 degrees relative to conventional dispersion plots. For this reason one should also study the following plot, which is identical except for being rotated, and is annotated as an aid to comprehension. Subsequent plots have the present orientation, however.

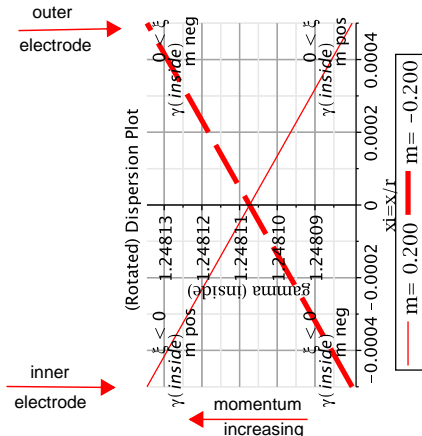


Figure: This plot is identical to the previous one except for being rotated by 90 degrees into conventional orientation (except momentum increases from right to left). It shows the dependence of $\xi = x/r$ vs "inside" gamma value γ^I , for $m = -0.2$ and $m = 0.2$. Note that, for $m < 0$ larger momentum causes larger radius while, for $m > 0$ the opposite is true. *What is striking is that the slope is opposite for $m > 0$ and $m < 0$. This is "anomalous".*

24 Potential energy

- ▶ Electric potential is defined to vanish on the design orbit
- ▶ Expressed as power series in ξ , the electric potential is

$$\begin{aligned} V(r) &= -\frac{E_0 r_0}{m} \left((1 - \xi)^m - 1 \right) \\ &= E_0 r_0 \left(\xi + \frac{1 - m}{2} \xi^2 + \frac{(1 - m)(2 - m)}{6} \xi^3 \dots \right). \end{aligned} \quad (1)$$

- ▶ This simplifies spectacularly for the Kepler $m=1$ case. But we are concerned with the small $|m| \ll 1$ case.
- ▶ As a proton orbit passes at right angles from outside to inside a bend element, its total energy is conserved;

$$\begin{aligned} \gamma^O(\xi) &= \frac{\mathcal{E}^O}{m_p c^2} = \frac{\mathcal{E}^I}{m_p c^2} \\ &= \gamma^I(\xi) + \frac{E_0 r_0}{m_p c^2 / e} \left(\xi + \frac{1 - m}{2} \xi^2 + \frac{(1 - m)(2 - m)}{6} \xi^3 \dots \right). \end{aligned}$$

- ▶ Plots of $\gamma^O(\xi)$ for $m = \pm 0.2$ are shown next

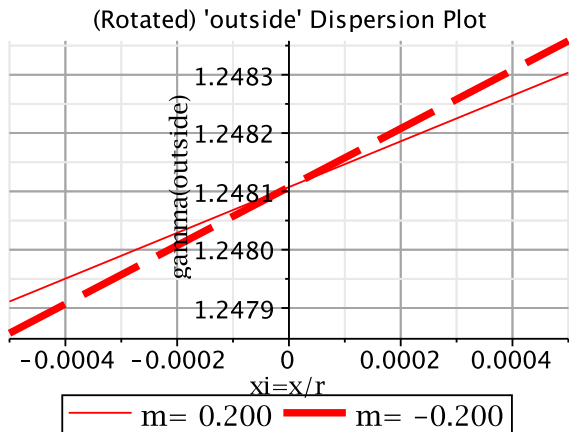


Figure: "Outside" dispersion plots. *Note that dispersion slopes are the same for $m < 0$ and $m > 0$. Dependence of "outside" gamma value γ^O on $\xi = x/r$ for $m = -0.2$ and $m = 0.2$. Because $d\gamma/d\beta = \beta\gamma^3$ is equal to about 1.17 at the magic proton momentum, the fractional spreads in velocity, momentum, and gamma are all comparable in value—in this case about 2×10^{-4} . The fractional spreads are an of magnitude greater outside than inside. This is helpful.*

26 Ultraweak focusing

- ▶ Figures so far have had $m = \pm 0.2$, which is actually *strong* focusing.
- ▶ From now on we assume *ultraweak* focusing with sector values alternating between $m = -0.002$ and $m = 0.002$. The dispersion plots are repeated.

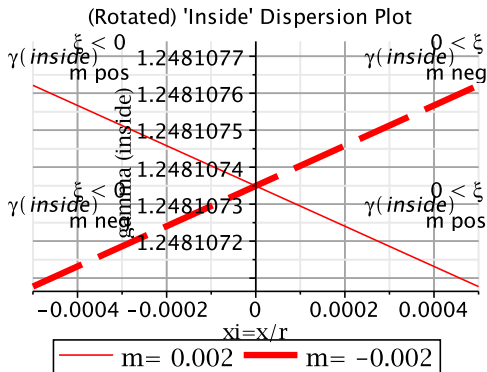


Figure: Dependence of “inside” gamma value γ^I on $\xi = x/r$ for $m = -0.002$ and $m = 0.002$. The curves intersect at the magic value $\gamma^I = 1.248107349$. Because $d\gamma/d\beta = \beta\gamma^3$ is equal to about 1.17 at the magic proton momentum, the fractional spreads in velocity, momentum, and gamma are all comparable in value—in this case about $\pm 3 \times 10^{-7}$ —a gloriously small range.

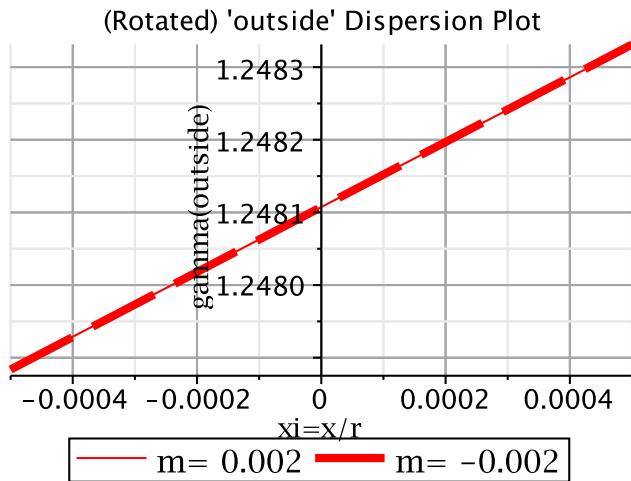


Figure: Dependence of “outside” gamma value γ^O on $\xi = x/r$ for $m = -0.002$ and $m = 0.002$. Because $d\gamma/d\beta = \beta\gamma^3$ is equal to about 1.17 at the magic proton momentum, the fractional spreads in velocity, momentum, and gamma are all comparable in value—in this case about $\pm 2 \times 10^{-4}$. *The fractional spreads are about three orders of magnitude greater outside than inside.*

28 Parameter table

Table: Parameters for WW-AG-CF proton EDM lattice

parameter	symbol	unit	value
arcs			2
cells/arc	N_{cell}		20
bend radius	r_0	m	40.0
drift length	L_D	m	4.0
circumference	C	m	411.327
field index	m		± 0.002
horizontal beta	β_x	m	40
vertical beta	β_y	m	1620
(outside) dispersion	D_x^O	m	24
horizontal tune	Q_x		1.640
vertical tune	Q_y		0.04045
number of protons	N_p		2×10^{10}
95% horz. emittance	ϵ_x	μm	3
95% vert. emittance	ϵ_y	μm	1
(outside) mom. spread	$\Delta p^O/p_0$		$\pm 2 \times 10^{-4}$
(inside) mom. spread	$\Delta p^I/p_0$		$\pm 2 \times 10^{-7}$

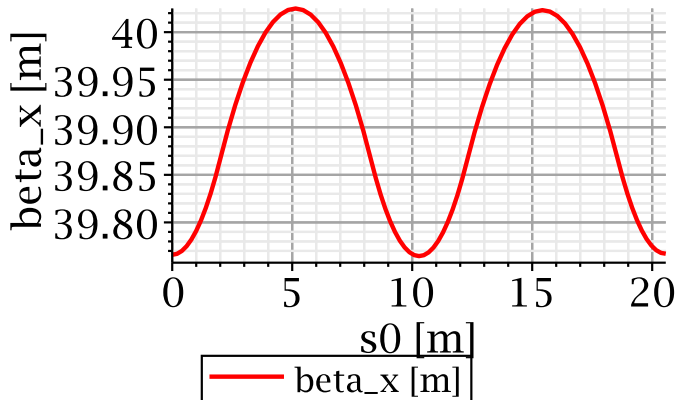


Figure: Horizontal beta function $\beta_x(s)$, plotted for two adjacent cells.

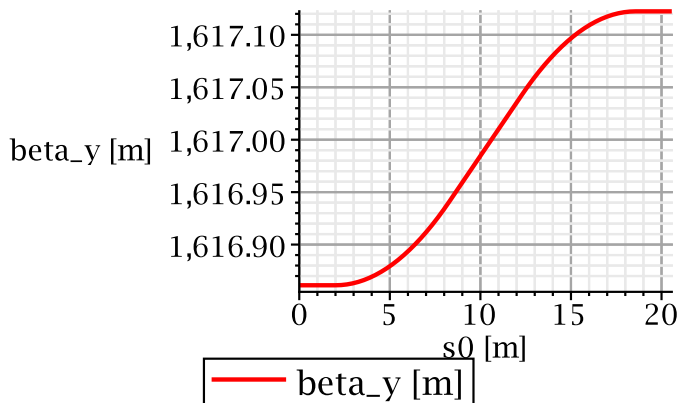


Figure: Vertical beta function $\beta_y(s)$, plotted for two adjacent cells. For this case the total circumference is 411.3 m and the total drift length is 160.0 m. Extended decimal places exhibit the extreme uniformity.

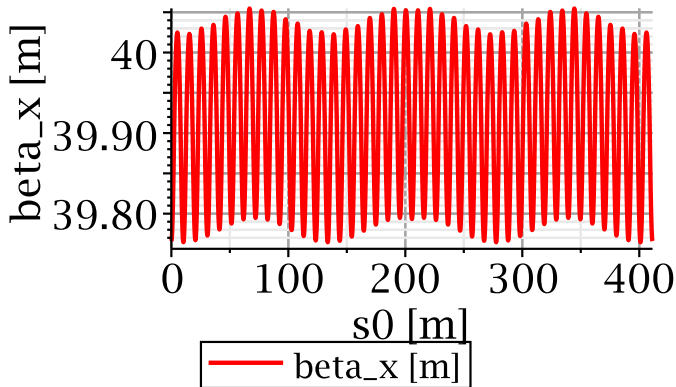


Figure: Horizontal beta function $\beta_x(s)$, plotted for full ring. For this case the total circumference is 411.3 m and the total drift length is $L_D=160.0$ m. Since this total drift length exceeds $L_D^{\text{trans.}}$, the ring will be “below transition”, as regards synchrotron oscillations.

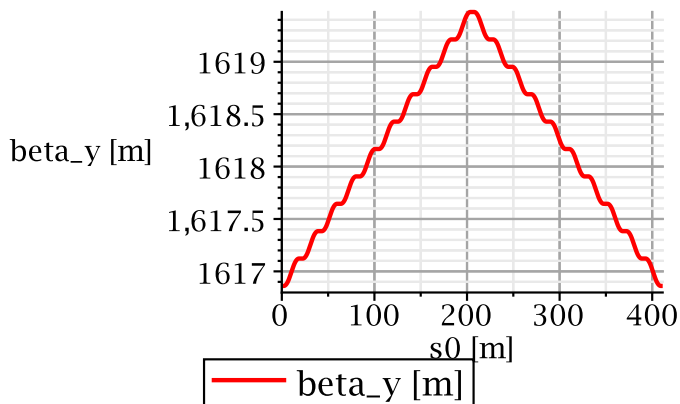


Figure: Vertical beta function $\beta_y(s)$, plotted for full ring. For this case the total circumference is 411.3 m and the total drift length is $L_D=160.0$ m. Since this total drift length exceeds $L_D^{\text{trans.}}$, the ring will be “below transition”, as regards synchrotron oscillations.

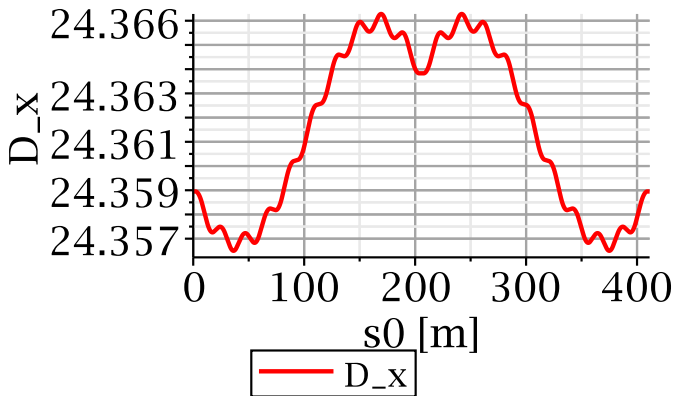


Figure: Outside dispersion function $D^O(s)$, plotted for full ring. For this case the total circumference is 411.3 m and the total drift length is 160.0 m. Extended decimal places exhibit the extreme uniformity.

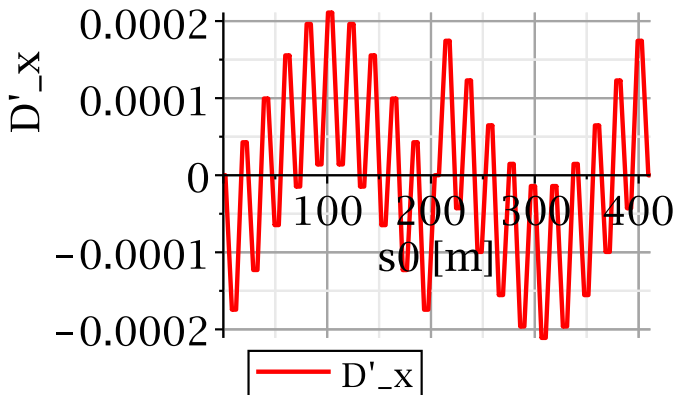


Figure: Outside dispersion function slope $D^o(s)'$, plotted for full ring. For this case the total circumference is 411.3 m and the total drift length is 160.0 m.

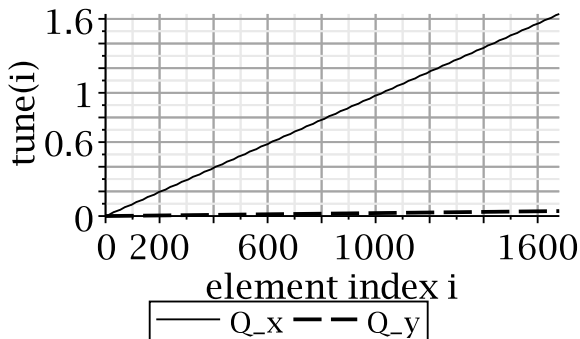


Figure: Transverse tune advances. The full lattice tunes are $Q_x = 1.640$ and $Q_y = 0.04046$. Even smaller horizontal tune (for improved self-magnetometry) can be provided by trim quadrupoles, rather than by electrode shape or voltage adjustment, even consistent with zero net quadrupole focusing, but with octupole focusing for net vertical stability.

36 *Self-magnetometry*

- ▶ The leading source of systematic error in the EDM measurement is unintentional, unknown, radial magnetic fields.
- ▶ Acting on MDM, they cause spurious precession mimicking EDM-induced precession.
- ▶ (Apart from eliminating radial magnetic field) the only protection is to measure the differential beam displacement of counter-circulating beams.
- ▶ Greatest sensitivity requires weakest vertical focusing.
- ▶ i.e. extremely large value for β_y .
- ▶ or even octupole-only vertical focusing.

37 Spin decoherence

In calculating spin decoherence we need to account for the transverse position oscillations accompanying potential energy variation. For simplicity we assume the lattice is uniform, with no drift regions. The spin precession angle α , relative to the proton direction, evolves as

$$\frac{d\alpha}{dt} = \frac{eE(x)}{m_p c} \left(\frac{g\beta(x)}{2} - \frac{1}{\beta(x)} \right).$$

The variables β , γ , and E in this equation depend on x (and also, though far less so, on y). But angular momentum L is conserved, and

$$\frac{d\theta}{dt} = \frac{L}{\gamma m_p r^2};$$

(which is valid in bend regions, but would not be in drift regions, where r becomes ambiguous). In this equation the angular momentum L is a constant of the motion (because the force is radial) but γ and $r = r_0 + x$ depend on x . Combining the two previous equations,

$$\frac{d\alpha}{d\theta} = \frac{eE(x)(r_0 + x)^2}{Lc\beta(x)} \left(\left(\frac{g}{2} - 1 \right) \gamma(x) - \frac{g/2}{\gamma(x)} \right),$$

- ▶ To find the evolution of α over long times, for an individual particle, we need to average this equation over betatron and synchrotron oscillations.
- ▶ What makes this averaging difficult is the fact that the final factor has, intentionally, been “magically” arranged to cancel for the central, design particle.
- ▶ The initial factor, though not constant, varies over a quite small range. A promising approximation scheme for this factor is to neglect the (small) rapidly oscillating betatron contribution to x coming from the betatron oscillation, and retain only the off-momentum part $x = D_x \Delta \gamma^0$ associated with the slowly varying synchrotron oscillation.
- ▶ Then the average excess precession for an off-momentum particle is

$$\left\langle \frac{d\alpha}{d\theta} \right\rangle (\gamma^0) = \frac{eE(D_x \Delta \gamma^0)(r_0 + D_x \Delta \gamma^0)^2}{Lc\beta(D_x \Delta \gamma^0)} \left\langle \left(\frac{g}{2} - 1 \right) \gamma(x) - \frac{g/2}{\gamma(x)} \right\rangle.$$

- ▶ The superscript “0” on $\gamma(x)$ is now just implicit in the final factor since only “inside” motion is under discussion.
- ▶ If the average of $\langle \gamma \rangle$ were the inverse of $\langle 1/\gamma \rangle$ the averaging over horizontal betatron oscillation would be easy. But this is not true.
- ▶ However the factorization has allowed the averaging over γ^0 to be deferred.

39 Virial theorem decoherence calculation

- ▶ The virial theorem can be used to perform 3D averages over multiparticle systems subject to central forces.
- ▶ Also, though our electric field is centrally directed within any single deflecting element, because of drift regions in the lattice, the centers of the various deflection elements do not coincide.
- ▶ We can therefore calculate only the spin decoherence applicable to passage through the bend regions, which is where the overwhelmingly dominant part of the momentum evolution occurs.
- ▶ The independent variables θ and t are very nearly, but not exactly proportional to each other instantaneously, so averages with respect to one or the other are not necessarily identically instantaneously.
- ▶ However, with bunched beams over long times, θ and t are strictly proportional (on the average) and the two forms of averaging have to be essentially equivalent.
- ▶ Because there are so many variants of “the virial theorem” it is easier to derive it from scratch than to copy it from one of many possible references.

40 The “virial” G is defined, in terms of radius vector \mathbf{r} and momentum \mathbf{p} , by

$$G = \mathbf{r} \cdot \mathbf{p}$$

Our electric field is

$$\mathbf{E} = -E_0 \left(\frac{r_0}{r} \right)^{1+m} \hat{\mathbf{r}},$$

and Newton’s law gives

$$\frac{d\mathbf{p}}{dt} = e\mathbf{E}.$$

In a bending element the time rate of change of \mathbf{G} is given by

$$\begin{aligned} \left. \frac{dG}{dt} \right|_{\text{bend}} &= \dot{\mathbf{r}} \cdot \mathbf{p} + \mathbf{r} \cdot \dot{\mathbf{p}} \\ &= m_p \gamma v^2 - eE_0 \frac{r_0^{1+m}}{r^m} \\ &= m_p c^2 \gamma - m_p c^2 \frac{1}{\gamma} - eE_0 r_0 \frac{r_0^m}{r^m}. \end{aligned}$$

Averaging over time, presuming bounded motion, and therefore requiring $\langle dG/dt \rangle$ to vanish, one obtains

$$\left\langle \frac{1}{\gamma} \right\rangle = \langle \gamma \rangle - \frac{E_0 r_0}{m_p c^2 / e} \left\langle \frac{r_0^m}{r^m} \right\rangle.$$

This provides the needed relation between $\langle \gamma \rangle$ and $\langle 1/\gamma \rangle$.

41 Applying this result to perform the (time)-average yields

$$\left\langle \frac{d\alpha}{d\theta} \right\rangle = \frac{eE(D_x \Delta\gamma^O)(r_0 + D_x \Delta\gamma^O)^2}{Lc\beta(D_x \Delta\gamma^O)} \left(-\langle \gamma \rangle + \frac{g}{2} \frac{E_0 r_0}{m_p c^2 / e} \left\langle \frac{r_0^m}{r^m} \right\rangle \right).$$

For specializing this result to frozen spin $\gamma = \gamma_0$ operation, the following formulas, can be employed:

$$\begin{aligned} \gamma(x) &\equiv \gamma_0 + \Delta\gamma, \\ \frac{E_0 r_0}{m_p c^2 / e} &= \gamma_0 - \frac{1}{\gamma_0}, \\ \frac{r_0^m}{r^m} &\approx 1 - m \frac{x}{r_0}, \\ \gamma_0 &= \frac{g}{2} \left(\gamma_0 - \frac{1}{\gamma_0} \right). \end{aligned}$$

- ▶ These formulas assume the beam centroid energy and the storage ring lattice are exactly “magic”. If not true the average spin orientation would change systematically. What is being calculated is the spin orientation spreading.
- ▶ For perfectly sinusoidal synchrotron oscillations, the initial factor can be replaced by its average value. This yields

$$\left\langle \frac{d\alpha}{d\theta} \right\rangle \approx -\frac{E_0 r_0^2}{\beta_0 Lc/e} \left(\langle \Delta\gamma^I \rangle + \frac{g}{2} \frac{m}{r_0} \left(\gamma_0 - \frac{1}{\gamma_0} \right) \langle x \rangle \right).$$

(The superscript “I” has been restored as a reminder that $\Delta\gamma^I$ is evaluated within bend elements, as contrasted to within drift sections.) The numerical value of the leading factor is about 1.

- ▶ Copying the final equation from the previous slide, evaluating the leading factor on the design orbit, and dropping the negative sign, the decoherence rate is

$$\left\langle \frac{d\alpha}{d\theta} \right\rangle = \langle \Delta\gamma' \rangle + \frac{g}{2} m \left(\gamma_0 - \frac{1}{\gamma_0} \right) \frac{\langle x \rangle}{r_0}.$$

- ▶ Typical values for the relevant quantities are

$$\begin{aligned} m &= \pm 0.002, \\ \frac{x}{r_0} &= \frac{0.01}{40} \approx 3 \times 10^{-4} \\ \gamma' &= 3 \times 10^{-7} \end{aligned}$$

- ▶ Small as they are, to linear approximation each of these averages to zero. To following order

$$\left\langle \frac{d\alpha}{d\theta} \right\rangle \sim (3 \times 10^{-7})^2 + \frac{g}{2} 4 \times 10^{-6} \left(\gamma_0 - \frac{1}{\gamma_0} \right) (3 \times 10^{-4})^2.$$

- ▶ Decoherence in bend fringe fields is likely to be greater than this, but it also cancels if care is taken to assure linear synchrotron oscillations.

- ▶ We have shown, therefore, for the WW-AG-CF lattice, that decoherence in the bend regions can be neglected even in the presence of horizontal betatron oscillations,
- ▶ We have previously argued that decoherence associated with vertical betatron oscillation can also be neglected.
- ▶ As already mentioned, very long spin coherence times have been demonstrated for deuterons in the COSY storage ring in Juelich, Germany, though only after quite delicate adjustment of nonlinear elements in the ring. And COSY is a strong focusing ring for which spin decoherence can be expected to be far greater than in our weak focusing WW-AG-CF lattice.
- ▶ If beam bunches can survive for days their polarization states can probably survive as well.

- ▶ Kepler, Newton, 1650, Lagrange 1800, virial averaging: calculation has been described in several slides
- ▶ Modern computer programs: (unsuccessful) calculation has taken 8 years and counting
- ▶ What gives Newton, Lagrange the advantage?

44 Current situation in Juelich

- ▶ Many significant advances:
 - ▶ Highly polarized beam
 - ▶ electron cooling
 - ▶ stochastic cooling
 - ▶ phase locked beam polarization
- ▶ They have a 200 m magnetic ring and have demonstrated the ability to measure proton EDM to quite high accuracy except
- ▶ What they need is a 450 electric ring

46 Solution?

- ▶ Smash all computers—probably a good idea, but has to be rejected—it doesn't help with EDM experiment
- ▶ Computers make us dumber—probably—but that just makes EDM experiment harder
- ▶ Computers damage our spirit of adventure and self-confidence— surely this is the correct explanation.

47 Coincidences






Experiments that “could not be done”

- ▶ Aachen: first RF accelerator
- ▶ Frankfurt: Stern-Gerlach experiment
- ▶ Bonn: neutron storage ring
- ▶ Juelich: phase-locked beam polarization

Coincidence? all in the “same” place—central Rhine—must be the water

- ▶ Should be designated “Cultural heritage treasure”
- ▶ Physics is “culture”
- ▶ Politicians can understand this

48 Bibliography

-  R. Talman, *The Electric Dipole Moment Challenge*, IOP Publishing, 2017
-  R. and J. Talman, *Symplectic orbit and spin tracking code for all-electric storage rings*, Phys. Rev. ST Accel Beams **18**, ZD10091, 2015
-  R. and J. Talman, *Electric Dipole Moment Planning with a resurrected BNL Alternating Gradient Synchrotron electron analog ring*, Phys. Rev. ST Accel Beams **18**, ZD10092, 2015
-  R. Talman and J. Talman, *Octupole focusing relativistic self-magnetometer electric storage ring bottle*, arXiv:1512.00884-[physics.acc-ph], 2015
-  C. Møller, *The Theory of Relativity*, Clarendon Press, Oxford, 1952